HHS Public Access

Author manuscript

Methods Enzymol. Author manuscript; available in PMC 2016 February 24.

Published in final edited form as:

Methods Enzymol. 2015 ; 552: 211–228. doi:10.1016/bs.mie.2014.11.029.

Clocks and cardiovascular function

Sarah C. McLoughlin, **Philip Haines**, and **Garret A. FitzGerald**

Institute for Translational Medicine and Therapeutics, Smilow Center for Translational Research, Perelman School of Medicine, University of Pennsylvania, Philadelphia, PA 19104, USA

Abstract

Circadian clocks in central and peripheral tissues enable the temporal synchronization and organization of molecular and physiological processes of rhythmic animals, allowing optimum functioning of cells and organisms at the most appropriate time of day. Disruption of circadian rhythms, from external or internal forces, leads to widespread biological disruption and is postulated to underlie many human conditions, such as the incidence and timing of cardiovascular disease. Here, we describe *in vivo* and *in vitro* methodology relevant to studying the role of circadian rhythms in cardiovascular function and dysfunction

Keywords

Circadian rhythms; clocks; cardiovascular function; BMAL1; atherosclerosis; inflammation; thrombosis; blood pressure

Introduction

Our modern, 24-hour society generates considerable challenges to the optimal orchestration of biology by our internal circadian rhythms. The consequences are perhaps reflected in part by the higher incidences of cardiovascular disease, obesity, metabolic syndrome and cancer associated with shift work (Karlsson, Knutsson, & Lindahl, 2001; Stevens, 2009; Yang et al., 2013). Clinical interest is peaked by the timing of the occurrence of many human diseases, such as myocardial infarction and death from sepsis (Hastings, Reddy, & Maywood, 2003). A wide range of phenotypes arise from animal models of circadian disruption by genetic or environmental means, including cardiovascular disease, cancer, aging, abnormal inflammation and metabolism (Yang et al., 2013). The many mechanisms by which clock dysfunction results in such a variety of biological defects remain to be fully elucidated.

Autoregulatory transcriptional and translational feedback loops generate daily rhythms in gene transcription, translation and post-translational modifications (Bass & Takahashi, 2010). Rhythmic expression of clock-controlled genes (ccgs) is maintained by the positive limb core clock genes *Bmal1*, *Clock* and *Npas2* driving expression of E-box-containing genes, including *Per1/2*, *Cry1/2*, *Ror* and *Rev-erb* which negatively feedback to inhibit NPAS2/CLOCK:BMAL1function (Yang et al., 2013). The so-called “master clock” of the suprachiasmatic nucleus (SCN) entrains clocks in the periphery, while other signals, such as feeding or activity, enable peripheral clocks to cycle independently of the SCN (Damiola et al., 2000). Up to half of all protein coding genes cycle, generally in a tissue specific manner

(Zhang, Lahens, Ballance, Hughes, & Hogenesch, 2014). The extent of clock control is reflected in the variety of phenotypes reported in mouse models of genetic clock disruption. To date, such studies have been conducted with prenatal disruption of the gene of interest. However, as several adult diseases, such as cardiovascular disease, diabetes, hypertension, may have origins *in utero* (Barker, 1998), the phenotypes of prenatal clock disrupted mice may be partially due to the embryonic insult rather than clock disruption in adulthood. The effect of *in utero* clock disruption on adult diseases, as opposed to the effects of acute clock disruption in adulthood, is an unexplored but potentially important aspect of circadian biology and health that can be addressed by comparison of conventional knockouts (KOs) with postnatal, inducible KO models.

Cardiovascular events exhibit diurnal patterns of incidence which are mirrored in the peaks and troughs of various components of the cardiovascular system, including the renin–angiotensin system, QT interval, the pressor response to infused vasoconstrictors, sympathetic nerve activity, plasma fibrinolytic activity, platelet aggregability, and vascular contractility (Curtis et al., 2007; Doi et al., 2010; Jeyaraj et al., 2012; Paschos & FitzGerald, 2010; Reilly, Westgate, & FitzGerald, 2007; Westgate et al., 2008). Rhythms in blood pressure, endothelial function and the response to thrombogenic stimuli are abnormal in mouse models of clock disruption, as is the development of hypertension (Curtis et al., 2007; Doi et al., 2010; Westgate et al., 2008). As humans and mice are anti-phasic in their daily activities, it is unsurprising that their circadian rhythms in cardiovascular function are similarly reversed (Fig. 1).

There is now mounting *in vivo* and *in vitro* evidence demonstrating the presence of circadian rhythms in myocardial structure and function, indicating a role for cardiac clock function in myocardial contractility, electrophysiology, metabolism, remodeling (including myocyte hypertrophy and fibrosis), heart failure, and in the myocardium's response to stress including ischemia and hypertension (Bray et al., 2008; Durgan & Young, 2010; Martino & Sole, 2009). Studies using global and cardiomyocyte-specific knockout mouse models subjected to various pathologic stress states have demonstrated significant myocardium specific attenuation of time-of-day oscillations in circadian clock genes, changes in myocardial tissue/histology remodeling, function, metabolism, gene and protein expression. Studies have also demonstrated electrophysiological abnormalities in clock gene KO mice which may provide a biological basis for the clinically observed circadian rhythmicity of arrhythmias and sudden cardiac death (SCD) in human populations. Inducible cardiac-specific Bmal1 KO mice were shown to have several baseline EKG abnormalities, and arrhythmias were more readily induced in isolated hearts from these mice.

The influence of circadian rhythms on metabolism is pervasive and extends to the consequences of abnormal metabolism and nutrient levels, for example diabetes, hyperlipidemia and atherosclerosis. *Bmal1* KO mice display impaired glucose and lipid metabolism (Lee et al., 2011; Marcheva et al., 2010; Rudic et al., 2004), while $Clock^{\Delta 19/\Delta 19}$ mutant mice show hypercholesterolemia, increased macrophage uptake of modified lipoproteins, reduced macrophage cholesterol efflux, and increased atherosclerotic lesions (Pan, Jiang, & Hussain, 2013). Given the high incidence of cardiovascular disease and obesity, not only in shift workers but also in the general population at risk of “social jet lag”

(Karlsson et al., 2001), understanding the circadian contributions to such pathways is of great importance.

Circadian analysis of physiological parameters with radiotelemetry

Radiotelemetry allows continuous monitoring of various parameters of mouse physiology in a freely moving, unrestrained animal. It is ideal for circadian analysis of, for example, heart rate, blood pressure, locomotion or temperature, depending on the type of sensory probes implanted (Fig. 1) (Westgate et al., 2008). It far exceeds other methods such as tail cuff measurement of blood pressure or rectal temperature readings that require restraint and cannot be continuously assayed over time. A catheter implanted into the arterial lumen senses the intra-arterial pressure and conveys the information to a transmitter implanted in the abdomen or subcutaneously. Sensor probes implanted intraperitoneally or subcutaneously can also record temperature, heart rate and locomotion (Westgate et al., 2008). From our experience, mice recover well within 1 week of surgery and blood pressure returns to normal after 10 days.

For implantation of sensors to monitor blood pressure, mice are anesthetized with ketamine (100 mg/kg) and xylazine (100 mg/kg) and aseptically prepared. Surgery is performed under strict sterile conditions with all tools sterilized by autoclaving and alcohol wipes. The mouse is shaved on the surgery site and the skin is sterilized with alcohol and iodine. A horizontal incision of 1 cm is made in the neck and the telemetry catheter (a 5-cm, fluid-filled catheter, OD 0.4 mm, Data Sciences International, St Paul, MN) is inserted into the aortic or carotid lumen and the catheter is secured. The transmitter (TA11PA-F10/TA-F10, weight 1.5 g) is implanted either subcutaneously or in the peritoneal cavity for the carotid artery or abdominal aortic catheters, respectively. The incision is closed with 5-0 monofilament sutures and bacitracin ointment is applied topically. The mouse is allowed to recover on a heating pad, intraperitoneally injected with burenophrine (0.05 mg/kg) and then placed singly in a recording box. Telemetry recordings begin once the mice have healed after surgery, approximately after 1 week.

Primary cell culture of macrophages

Primary cell culture can be a source of information about a cell type or biological process that an immortalized cell line cannot provide due to its adjusted nature. Additionally, primary cultures can be derived from transgenic, KO or drug- or diet-treated animals. In our studies, one such cell is the peritoneal macrophage.

Peritoneal macrophage culture

Peritoneal cells can be harvested by peritoneal lavage and analyzed directly. Resident macrophages make up approximately 30%, while approximately 50% are B cells and 5-10% are T cells (Ray & Dittel, 2010). An enriched population of macrophages can be obtained by FACS analysis of peritoneal cells (Keller et al., 2009). Alternatively, the lavaged cells can be directly cultured as adherent cells for several days to obtain an enriched macrophage population and allowing, for example, synchronization for circadian experiments. Mice can be treated with thioglycollate to recruit naive macrophages to the cavity to increase the number of macrophages within the peritoneal cavity before harvest. An un-elicited harvest

of resident macrophages can result in approximately 1×10^6 cells per mouse, while thioglycollate can yield up more than five times that number. Note that the recruited, naive macrophages are not phenotypically the same as resident peritoneal macrophages and so may provide different results. Mice are interperitoneally injected with 0.5–0.8 mL of 10% thioglycollate 4 days prior to harvest to recruit macrophages to the peritoneal cavity(Hui et al., 2010). At the appropriate time points on harvest day, the mouse is anaesthetized and euthanized via CO_2. Cervical dislocation is not recommended due the risk of damage to the peritoneal cavity and leaking of blood. Five milliliters of ice cold, sterile phosphate buffered saline (PBS) is slowly injected into the peritoneal cavity, taking care to avoid the bladder and to insert the needle into the cavity and avoiding injecting the fluid into the subcutaneous area. To suspend the cells within the PBS, the mouse is gently agitated for up to a minute.

The skin is removed from the abdomen and the mouse is laid on one side with the peritoneum intact. The exposed peritoneal membrane is raised with a sterile forceps to a point and pierced carefully with a sterile scissors. The liquid is removed from the cavity with a pipette and placed into a tube on ice. Approximately 80% of the injected liquid can be recovered. Cells are centrifuged at $1000 \times g$ for one minute at 4°C. In a sterile tissue culture hood, the supernatant is removed and the cell pellet can be flash frozen or gently resuspended in the appropriate solution. For protein or RNA analysis, cells are resuspended in the appropriate lysis buffer. To culture the cells, the pellet is resuspended in culture medium (RPMI 1640, 1% penicillin/streptomycin, 10% FBS, 1% L-Glutamine) and the cells are plated into tissue culture dishes and incubated at 37°C in 5% CO_2 for up to 5 days with medium changes every other day. The resulting adherent cells are peritoneal macrophages and can be administered various treatments, including synchronization with 100 nM dexamethasone to synchronize the circadian rhythms of the cells (Fig. 2).

Bone marrow-derived macrophages

A source of large numbers of macrophages and other immune cells is the bone marrow. Bone marrow can be harvested from the femurs of mice and cultured to allow differentiation and proliferation of macrophages, mast cells or other immune cells, depending on the culture conditions.

The mouse is anaesthetized and euthanized via CO2 and cervical dislocation if appropriate. The hind limb is stripped of skin. Using a sterile scissors, the hind limb is cut away from the torso at the hip joint, taking care not to break the femur. The femur is carefully separated from the lower limb and the bone is cleaned of muscle, tendon etc. within a sterile tissue culture hood using sterile forceps and small scissors. Once the femur is cleared of tissue, a syringe and 25 gauge needle is used to force 10 ml of medium through the distal femur head. Bone marrow is flushed from the femur into a tube (medium consists of DMEM with 10% FCS, 1% penicillin/streptomycin and 1% L-Glutamine). If necessary, the proximal head of the femur can also be pierced with the needle to ensure flow through. The bone marrow is mixed gently in the medium by pipetting then collected by centrifugation at 1500 rpm for 5 min at room temperature. At this stage, the pelleted bone marrow can be resuspended in DMEM with 50 % FCS and frozen at − 80°C until required. Alternatively, the pellet is resuspended in 20 mL of medium then filtered through a cell strainer into a 50 mL tube. The

cell solution is centrifuged again at 1500 rpm for 5 min and the resulting pellet is resuspended in 10 mL LCCM (see below for details). The cells are counted and plated at a concentration of 1×10^6 cells per milliliter into sterile tissue culture plates and cultured overnight at 37°C. Every 4 days after, medium is replaced with LCCM. After 8 days, macrophages have differentiated and can be used in experiments such as synchronization with 100 n*M* dexamethasone. The medium for differentiation of macrophages from bone marrow, LCCM, can be obtained from the medium of cultured L929 which contains colony stimulating factor 1 (CSF1). L929 cells are cultured in DMEM with 10 % FBS, 1 % penicillin/streptomycin and 1 % L-Glutamine. When cells are confluent, the medium is harvested, centrifuged at 2000 rpm for 5 min at room temperature, and the supernatant is frozen until required. The resulting solution is diluted 1:5 in DMEM full medium to obtain LCCM for macrophage differentiation.

Circadian variation in thrombogenesis

Diurnal variations occur in the cardiovascular system, including changes in heart rate and blood pressure (Fig. 3) (Reilly et al., 2007; Westgate et al., 2008), while cardiovascular clinical events, such as myocardial infarction and stroke, are more prevalent at particular times of the day (Yang et al., 2013). Clock genes play a central role in the normal functioning of the cardiovascular system and the timing of its various components. We have previously described *in vivo* a diurnal variation in response to a thrombogenic stimulus with a peak at ZT8. This pattern is disrupted in mouse models of abnormal circadian rhythms ($Clock^{d19}$ mutants and *Bmal1* and *Npas2* KOs) (Westgate et al., 2008). In humans, thrombogenesis peaks in the morning. Platelet surface activation markers are most present in the morning, coinciding with the peak in myocardial infarction and stroke and antiphase to plasminogen activator inhibitor-1 (*Pai-1*) (Yang et al., 2013). Methods such as the time to vessel occlusion (TTVO) model and real-time fluorescence intravital microscopy can be used to further investigate the roles of the clock and of non-clock genes in the timing of cardiovascular events.

Time to vessel occlusion (TTVO)

The photosensitizing dye, Rose Bengal, produces reactive oxygen species when exposed to green light and is used in thrombotic studies of the microvasculature – such as in carotid or femoral arteries - where it induces focal vascular injury by endothelial damage without an intra-arterial line, resulting in thrombosis (Westrick, Winn, & Eitzman, 2007). Mice are anesthetized with ketamine (100 mg/kg), xylazine (10 mg/kg) and acepromaxine (1 mg/Kg) in 0.9% saline and maintained on a 37°C heating pad. The right common carotid artery or the femoral artery can be the site of injury. The artery is exposed and a Doppler flow probe is attached. The flow probe allows monitoring of blood flow in real time. A 1.5-mW green light laser (540 nm) is trained on the intended site of injury on the exposed carotid artery. Rose Bengal is injected into the jugular vein (50 mg/kg). Flow in the vessel of interest is monitored by the Doppler probe from the onset of injury. TTVO is measured as the time between administration of Rose Bengal and cessation of blood flow in the artery for at least 3 min.

Real-time fluorescence intravital microscopy quantification of thrombosis

While TTVO provides information on flow within the vessel, visualization of thrombus formation provides additional information on the kinetics of thrombus formation and changes in the participating cell types (Kim, Barazia, & Cho, 2013) which may be affected by the circadian system. Real-time fluorescence intravital microscopy of the cremaster muscle vasculature is a powerful method whereby response to vascular injury can be visualized in real time and the molecular expression of activated intravascular cells may be analyzed using antibodies specifically optimized for this use. Mice are anesthetized with an intraperitoneal injection of ketamine (100 mg/kg), xylazine (10mg/kg) and acepromaxine (1mg/Kg) and kept at 37°C using a thermal pad. The left jugular vein is exposed for administration of antibodies such as CD41, also known as integrin α2b and GPIIb, a transmembrane glycoprotein that is expressed by platelets and megakaryocyte. The scrotum is cut, exposing the cremaster muscle which is then pinned over the microscopy stage and bathed in a 37°C bicarbonate-buffered saline aerated with 95% N2 and 5% CO2. Digital images of thrombus formation are obtained with an Olympus BX61WI microscope and widefield fluorescence microscopy is performed with a 2-Galvo high-speed wavelength changer equipped with a high-intensity 300-W xenon light source. A Hamamatsu C9300-201 charge-coupled device (CCD) camera captures 20 frames per second for fluorochrome channels and a Hamamatsu image intensifier is used to amplify light up to 1000-fold for widefield imaging. Brightfield and fluorescent images are collected at the same time by using a Uniblitz shutter on the transmission light source that opens and closes in 50 m. A fluorescence resonance energy transfer/fluorescence recovery after photo-bleaching photo-ablation system is used to induce arteriolar injury. The laser is set to 440 nm, focused through the microscope objective, parfocal with the focal plane, and aimed at the vessel wall. Depending on the thickness of the cremaster preparation and the size of the vessel, a nitrogen dye laser pulses three to five times at 55-65% power. Successive thrombi are generated either upstream of the previous thrombus or in different arterioles within the same cremaster preparation. A total of 10 images from 10 thrombi are collected over approximately 1.5 h. For quantification of thrombosis, fluorescence intensity is measured for each image and corrected for background intensity as follows: mean background intensity of each image is calculated as the average pixel intensity in a defined region of the blood vessel just upstream of the injury and developing thrombus. The area of the thrombus is defined as the total number of pixels with fluorescence greater than the mean background intensity during the course of the image capture. Background fluorescence is corrected for by multiplying the mean background intensity by the area of the thrombus then subtracting from the total fluorescence intensity of the thrombus in each image. (Chen et al., 2013; Yu et al., 2012)

TTVO and real-time fluorescence intravital microscopy can be used to investigate the circadian aspects of normal and abnormal thrombosis and to further characterize the thrombogenic phenotypes of mouse models of circadian disruption.

Atherosclerosis and vascular integrity in models of clock disruption

Disruption of circadian rhythms has been shown to disrupt lipid metabolism and induce obesity (Paschos et al., 2012; Turek et al., 2005). *Bmal1* deletion in adipose tissue alone

leads to abnormal plasma lipid profiles (Paschos et al., 2012), while cholesterol metabolism is impaired in *Clock*$^{\Delta 19/\Delta 19}$ mutant mice resulting in hypercholesterolemia (Pan et al., 2013). Impairments include enhanced intestinal cholesterol absorption and increased uptake of modified lipoproteins and defective cholesterol efflux by macrophages from *Clock*$^{\Delta 19/\Delta 19}$ mutant mice. Increased atherogenesis and atherosclerosis were observed in these mice, leading to the conclusion that the circadian gene *Clock* is important in normal lipid metabolism and attenuates atherogenesis while disruption of circadian rhythms may increase atherosclerotic plaques and associated macrophage dysfunction. The effects of other core clock genes and non-genetic forms of circadian disruption on lipid metabolism and atherosclerosis require further investigation. Methods allowing analysis of atherosclerotic lesions (*en face* analysis), the integrity of the aorta (immunohistochemistry of aortic sections) are applicable to such studies.

The vascular response to mechanical intraluminal injury may reflect the likelihood of restenosis after angioplasty and also may reveal a propensity to the development of vascular disease. *Clock*$^{\Delta 19/\Delta 19}$ mutation or *Bmal1* KO results in an increase in intimal hyperplasia in response to intraluminal vascular injury, with an increase in neointimal area and intima-to-medial (I/M) ratio indicative of an exacerbated response to wire injury (Anea et al., 2009). Interestingly, the effect is only seen in clock-deficient animals housed in complete darkness (DD) but not in those in a regular light/dark cycle, highlighting a complicated relationship between vascular integrity, light cycles and the circadian clock. Analysis of the femoral artery after intraluminal wire injury in further models of clock disruption and light/dark cycles can contribute to our understanding of this relationship.

En face analysis of aortas

Preparation of the aorta for *en face* lesion analysis requires approximately 1 h. Mice are euthanized, and the aorta is exposed by dissecting away the anterior chest wall, heart, lungs and diaphragm, and carefully displacing the contents of the abdominal cavity laterally. The esophagus, positioned anteriorly to the aorta, is removed and the area around the aorta is cleared of adipose and connective tissues. The major branching arteries are dissected away. From the aortic root to the iliac bifurcation, the aorta is separated from the spinal cord and placed whole in formalin-free fixative Prefer (Anatech LTD). Any remaining adventitial fat or connective tissue is removed and the aorta is opened with a ventral, longitudinal cut along its length. The aorta is pinned out on a black wax-covered petri dish using 0.2-mm diameter stainless steel pins (Fine Science Tools) and stained with Sudan IV (Sigma). Atherosclerotic plaques are analyzed and quantified as the percentage of the lesion area to the intimal area (Phase 3 Imaging Systems).

Aortic root sectioning and staining

Mouse hearts including the aortic root are removed and embedded in optimum cutting temperature compound (OCT). Serial sections of 10 μm thickness of the aortic root are cut using a cryostat and mounted on slides. Sections are allowed air dry at room temperature for 5 min then fixed in acetone at − 20°C for 15 minutes, and 3% H_2O_2 for 15 min at room temperature (blocking treatment for endogenous peroxidase), 10% normal serum blocking solution in 1% BSA/PBS for 15 min (dependent on the host animal of the secondary

antibody) followed by streptavidin-biotin blocking kit as per manufacturers' instructions (Vector Laboratories) for endogenous biotin. Sections are then incubated with the chosen primary antibody in blocking solution overnight at 4°C. Sections can be individually stained for collagen type-I and laminin to identify fibrotic lesions; α-SMA, a marker of differentiated VSMCs; VCAM-1, a marker of proliferative VSMCs; or CD11b to identify inflammatory macrophages (Tang et al., 2014). Where required, sections are then incubated with biotinylated-IgG secondary antibody (specific to host of primary antibody) diluted in 1% BSA/PBS for 1 h at room temperature. Sections are then incubated with Streptavidin-Horseradish Peroxidase diluted in 1% BSA/PBS for 30 min at room temperature. Slides are equilibrated in sterile H_2O for 5 min at room temperature and developed using the DAB substrate kit (Dako). Sections are counterstained with hematoxylin, dehydrated and mounted. Isotype-matched controls are performed in parallel as negative controls to differentiate specific antibody signal from non-specific background signal. Isotype-matched controls should show negligible staining.

Wire-Mediated Vascular Injury

Mice are reversibly anaesthetized as described above. Blunt dissection exposes one side of the right femoral artery and carefully separates it from the adjoining femoral vein and nerve. Blood flow is ceased for the duration of the procedure by looping 6-0 silk suture proximally and distally around the femoral artery. A transverse arteriotomy is made in femoral artery in the branch between the rectus femoris and vastus medialis muscles and an angioplasty wire (Cook Inc) 0.35 mm in diameter is inserted into the arterial lumen toward the iliac artery. The wire is left in place for 3 min to ensure the artery is denuded and dilated. The wire is then removed and blood flow is restarted by removing the sutures looped on the artery and the skin incision closed with a 5-0 silk suture. As a control, the femoral artery of the left side is sham operated. The animals are sacrificed 28 days after injury for femoral artery harvest. Arteries are fixed in 4 % paraformaldehyde, paraffin-embedded and cross-sectioned for analysis. From the distal branch point, eight portions of the artery are sectioned with 200 μm between each portion. Sections from each portion are analysed by hematoxylin and eosin staining, immunohistochemistry and morophometric analysis. Data such as intima-to-media ratio and percentage stenosis can be obtained to determine response to vascular injury in further clock deficient mouse models, such as those of the negative limb, to provide a more complete picture of the interactions between the clock, light cycles and vascular injury (Anea et al., 2009; Sata et al.; M. Wang et al., 2011).

Clocks and myocardial dysfunction

Myocardial circadian studies have used several methodological approaches, some of which are unique for demonstrating a role for molecular clocks specifically in myocardial function, structure, and disease. These include the use of cardiac specific clock gene KO mice, the isolation of primary cardiomyocytes for *in vitro* studies, and the ability to fine phenotype *in vivo* heart structure and function using non-invasive techniques such as echocardiography and cardiac MRI.

Mouse echocardiography

A comprehensive mouse 2-dimensional (2-D) and Doppler echocardiogram is performed in anaesthetized mice using a mixture of 1-2 % isoflurane gas and 100 % oxygen which has relatively small effects on cardiovascular performance. The mouse is positioned supine on a heated platform and core temperature is maintained at 37 °C. An ECG signal is recorded through electrode pads and chest hair is removed using a chemical depilator (Nair) to minimize ultrasound attenuation. The ultrasound probe is positioned on the chest using warm gel between the probe head and the chest wall. 2-D images are recorded in the parasternal long- and short-axis views and M-mode recordings are obtained (Fig. 4 A and B). Left ventricular and left atrial cavity dimensions, wall thickness (measures of structural remodeling) and systolic function readouts (fractional shortening and ejection fraction) can be calculated using methods approved by the American Society of Echocardiography (Lang et al.) and software from specific vendors. Color Doppler is employed to identify transmitral flow and to estimate early and late diastolic peak velocities (E and A and E/A ratio) (Fig. 4 C). The transmitral diastolic waveform can be used to measure systolic intrevals (isovolumetric contraction time, ventricular ejection time) and diastolic intervals (isovolumetric relaxation time and acceleration and deceleration times of the E-wave (E_{AT} and E_{DT}) (Fig. 4C). Pulsed Doppler interrogations can be made in the 4-chamber view placing the sample volume over the septal wall at the mitral annulus to measure early myocardial tissue relaxation during diastole (Fig. 4 D)(Yuan, Wang, Liu, Cohen, & Patel, 2010).

Isolation of adult ventricular mouse cardiomyocytes

Mice are injected intraperitoneally with 100 U of heparin. Phenobarbital 50mg/kg is used and the hearts are excised via a sternotomy and placed on a Langendorf perfusion platform using Ca^{2+}-free Tyrode's solution for 6 min at 3.0-3.5 ml/min at 36-37 °C. The hearts are then perfused with Ca^{2+}-free Tyrode's solution with collagenase B and D (Roche) and protease (Fraction IV, Sigma) for 12-15 min. The hearts begin to adopt a pale and flaccid appearance. They are removed from the Langendorf platform and the ventricles are excised and placed in Ca^{2+}free Tyrode's solution with 1 mg/ml of bovine serum albumin . The ventricles are split into small pieces and triturated carefully using a Pasteur pipette to isolate individual myocytes, which can synchronized for circadian analysis and used for *in vitro* structure, function, electrophysiological phenotyping and mechanistic studies (Rentschler et al., 2012) (D. Wang et al., 2009).

Finally, nuclear cardiac imaging studies, invasive hemodynamic studies, and measurements of serum biomarkers of myocardial dysfunction (e.g. NT-Pro-BNP), damage (e.g. Troponin T and I), and fibrosis (Galectin-3) represent other *in vivo* approaches, which can be employed to demonstrate the presence of functionally relevant myocardial metabolic, hemodynamic, functional, and tissue derangements secondary to dysfunctional molecular clocks and/or circadian stressors.

Conclusion

Many aspects of the cardiovascular system are governed by circadian clock timing, and thus optimum functioning of the system is vulnerable to circadian disruptions. Much remains to be understood on the interplay among clocks, the cardiovascular system and their impact on the health of our socially jetlagged populations of shift workers and non-shift workers alike.

References

Anea CB, Zhang M, Stepp DW, Simkins GB, Reed G, Fulton DJ, Rudic RD. Vascular Disease in Mice With a Dysfunctional Circadian Clock. Circulation. 2009; 119(11):1510–1517. doi: 10.1161/circulationaha.108.827477. [PubMed: 19273720]

Barker DJ. In utero programming of chronic disease. Clin. Sci. 1998; 95(2):115–128. [PubMed: 9680492]

Bass J, Takahashi JS. Circadian Integration of Metabolism and Energetics. Science. 2010; 330(6009): 1349–1354. doi: 10.1126/science.1195027. [PubMed: 21127246]

Bray MS, Shaw CA, Moore MW, Garcia RA, Zanquetta MM, Durgan DJ, Young ME. Disruption of the circadian clock within the cardiomyocyte influences myocardial contractile function, metabolism, and gene expression. Am J Physiol Heart Circ Physiol. 2008; 294(2):H1036–1047. doi: 10.1152/ajpheart.01291.2007. [PubMed: 18156197]

Chen L, Yang G, Xu X, Grant G, Lawson JA, Bohlooly-Y M, FitzGerald GA. Cell Selective Cardiovascular Biology of Microsomal Prostaglandin E Synthase-1. Circulation. 2013; 127(2):233–243. doi: 10.1161/circulationaha.112.119479. [PubMed: 23204105]

Curtis AM, Cheng Y, Kapoor S, Reilly D, Price TS, FitzGerald GA. Circadian variation of blood pressure and the vascular response to asynchronous stress. Proceedings of the National Academy of Sciences. 2007; 104(9):3450–3455. doi: 10.1073/pnas.0611680104.

Damiola F, Le Minh N, Preitner N, Kornmann B. t. Fleury-Olela F, Schibler U. Restricted feeding uncouples circadian oscillators in peripheral tissues from the central pacemaker in the suprachiasmatic nucleus. Genes & Development. 2000; 14(23):2950–2961. doi: 10.1101/gad.183500. [PubMed: 11114885]

Doi M, Takahashi Y, Komatsu R, Yamazaki F, Yamada H, Haraguchi S, Okamura H. Salt-sensitive hypertension in circadian clock-deficient Cry-null mice involves dysregulated adrenal Hsd3b6. Nat Med. 2010; 16(1):67–74. doi: http://www.nature.com/nm/journal/v16/n1/suppinfo/nm.2061_S1.html. [PubMed: 20023637]

Durgan DJ, Young ME. The cardiomyocyte circadian clock: emerging roles in health and disease. Circ Res. 2010; 106(4):647–658. doi: 10.1161/CIRCRESAHA.109.209957. [PubMed: 20203314]

Hastings MH, Reddy AB, Maywood ES. A clockwork web: circadian timing in brain and periphery, in health and disease. Nature Reviews Neuroscience. 2003; 4:649–661. [PubMed: 12894240]

Hui Y, Ricciotti E, Crichton I, Yu Z, Wang D, Stubbe J, FitzGerald GA. Targeted Deletions of Cyclooxygenase-2 and Atherogenesis in Mice. Circulation. 2010; 121(24):2654–2660. doi: 10.1161/circulationaha.109.910687. [PubMed: 20530000]

Jeyaraj D, Haldar SM, Wan X, McCauley MD, Ripperger JA, Hu K, Jain MK. Circadian rhythms govern cardiac repolarization and arrhythmogenesis. Nature. 2012; 483(7387):96–99. [PubMed: 22367544]

Karlsson B, Knutsson A, Lindahl B. Is there an association between shift work and having a metabolic syndrome? Results from a population based study of 27 485 people. Occupational and Environmental Medicine. 2001; 58(11):747–752. doi: 10.1136/oem.58.11.747. [PubMed: 11600731]

Keller M, Mazuch J, Abraham U, Eom GD, Herzog ED, Volk H-D, Maier B. A circadian clock in macrophages controls inflammatory immune responses. Proceedings of the National Academy of Sciences. 2009; 106(50):21407–21412. doi: 10.1073/pnas.0906361106.

Kim KH, Barazia A, Cho J. Real-time Imaging of Heterotypic Platelet-neutrophil Interactions on the Activated Endothelium During Vascular Inflammation and Thrombus Formation in Live Mice. 2013; (74):e50329. doi: doi:10.3791/50329.

Lang RM, Bierig M, Devereux RB, Flachskampf FA, Foster E, Pellikka PA, Stewart WJ. Recommendations for Chamber Quantification: A Report from the American Society of Echocardiography's Guidelines and Standards Committee and the Chamber Quantification Writing Group, Developed in Conjunction with the European Association of Echocardiography, a Branch of the European Society of Cardiology. Journal of the American Society of Echocardiography. 18(12):1440–1463. doi: 10.1016/j.echo.2005.10.005. [PubMed: 16376782]

Lee J, Kim M-S, Li R, Liu VY, Fu L, Moore DD, Yechoor VK. Loss of Bmal1 leads to uncoupling and impaired glucose-stimulated insulin secretion in β-cells. Islets. 2011; 3(6):381–388. [PubMed: 22045262]

Marcheva B, Ramsey KM, Buhr ED, Kobayashi Y, Su H, Ko CH, Bass J. Disruption of the clock components CLOCK and BMAL1 leads to hypoinsulinaemia and diabetes. Nature. 2010; 466(7306):627–631. doi: http://www.nature.com/nature/journal/v466/n7306/abs/nature09253.html#supplementary-information. [PubMed: 20562852]

Martino TA, Sole MJ. Molecular time: an often overlooked dimension to cardiovascular disease. Circ Res. 2009; 105(11):1047–1061. doi: 10.1161/CIRCRESAHA.109.206201. [PubMed: 19926881]

McLoughlin SC, FitzGerald GA. Between a ROCK and a Hard Place: How to Align Our Circadian Rhythms? Circulation. 2013; 127(1):19–20. doi: 10.1161/circulationaha.112.150417. [PubMed: 23172837]

Pan X, Jiang X-C, Hussain MM. Impaired Cholesterol Metabolism and Enhanced Atherosclerosis in Clock Mutant Mice. Circulation. 2013; 128(16):1758–1769. doi: 10.1161/circulationaha.113.002885. [PubMed: 24014832]

Paschos GK, FitzGerald GA. Circadian Clocks and Vascular Function. Circulation Research. 2010; 106(5):833–841. doi: 10.1161/circresaha.109.211706. [PubMed: 20299673]

Paschos GK, Ibrahim S, Song W-L, Kunieda T, Grant G, Reyes TM, FitzGerald GA. Obesity in mice with adipocyte-specific deletion of clock component Arntl. Nat Med. 2012; 18(12):1768–1777. doi: http://www.nature.com/nm/journal/v18/n12/abs/nm.2979.html#supplementary-information. [PubMed: 23142819]

Ray A, Dittel BN. Isolation of Mouse Peritoneal Cavity Cells. 2010; (35):e1488. doi: doi:10.3791/1488.

Reilly DF, Westgate EJ, FitzGerald GA. Peripheral Circadian Clocks in the Vasculature. Arteriosclerosis, Thrombosis, and Vascular Biology. 2007; 27(8):1694–1705. doi: 10.1161/atvbaha.107.144923.

Rentschler S, Yen AH, Lu J, Petrenko NB, Lu MM, Manderfield LJ, Epstein JA. Myocardial Notch signaling reprograms cardiomyocytes to a conduction-like phenotype. Circulation. 2012; 126(9):1058–1066. doi: 10.1161/CIRCULATIONAHA.112.103390. [PubMed: 22837163]

Rudic RD, McNamara P, Curtis A-M, Boston RC, Panda S, Hogenesch JB, FitzGerald GA. BMAL1 and CLOCK, Two Essential Components of the Circadian Clock, Are Involved in Glucose Homeostasis. PLoS Biol. 2004; 2(11):e377. doi: 10.1371/journal.pbio.0020377. [PubMed: 15523558]

Sata M, Maejima Y, Adachi F, Fukino K, Saiura A, Sugiura S, Nagai R. A Mouse Model of Vascular Injury that Induces Rapid Onset of Medial Cell Apoptosis Followed by Reproducible Neointimal Hyperplasia. Journal of Molecular and Cellular Cardiology. 32(11):2097–2104. doi: 10.1006/jmcc.2000.1238. [PubMed: 11040113]

Stevens RG. Light-at-night, circadian disruption and breast cancer: assessment of existing evidence. International Journal of Epidemiology. 2009; 38(4):963–970. doi: 10.1093/ije/dyp178. [PubMed: 19380369]

Tang SY, Monslow J, Todd L, Lawson J, Puré E, FitzGerald GA. Cyclooxygenase-2 in Endothelial and Vascular Smooth Muscle Cells Restrains Atherogenesis in Hyperlipidemic Mice. Circulation. 2014; 129(17):1761–1769. doi: 10.1161/circulationaha.113.007913. [PubMed: 24519928]

Turek FW, Joshu C, Kohsaka A, Lin E, Ivanova G, McDearmon E, Bass J. Obesity and Metabolic Syndrome in Circadian Clock Mutant Mice. Science. 2005; 308(5724):1043–1045. doi: 10.1126/science.1108750. [PubMed: 15845877]

Wang D, Patel VV, Ricciotti E, Zhou R, Levin MD, Gao E, FitzGerald GA. Cardiomyocyte cyclooxygenase-2 influences cardiac rhythm and function. Proc Natl Acad Sci U S A. 2009; 106(18):7548–7552. doi: 10.1073/pnas.0805806106. [PubMed: 19376970]

Wang M, Ihida-Stansbury K, Kothapalli D, Tamby MC, Yu Z, Chen L, FitzGerald GA. Microsomal Prostaglandin E2 Synthase-1 Modulates the Response to Vascular Injury. Circulation. 2011; 123(6):631–639. doi: 10.1161/circulationaha.110.973685. [PubMed: 21282500]

Westgate EJ, Cheng Y, Reilly DF, Price TS, Walisser JA, Bradfield CA, FitzGerald GA. Genetic Components of the Circadian Clock Regulate Thrombogenesis In Vivo. Circulation. 2008; 117(16):2087–2095. doi: 10.1161/circulationaha.107.739227. [PubMed: 18413500]

Westrick RJ, Winn ME, Eitzman DT. Murine Models of Vascular Thrombosis. Arteriosclerosis, Thrombosis, and Vascular Biology. 2007; 27(10):2079–2093. doi: 10.1161/atvbaha.107.142810.

Yang G, Paschos G, Curtis AM, Musiek ES, McLoughlin SC, FitzGerald GA. Knitting Up the Raveled Sleave of Care. Science Translational Medicine. 2013; 5(212):212rv213. doi: 10.1126/scitranslmed.3007225.

Yu Y, Ricciotti E, Scalia R, Tang SY, Grant G, Yu Z, FitzGerald GA. Vascular COX-2 Modulates Blood Pressure and Thrombosis in Mice. Science Translational Medicine. 2012; 4(132):132ra154. doi: 10.1126/scitranslmed.3003787.

Yuan L, Wang T, Liu F, Cohen ED, Patel VV. An evaluation of transmitral and pulmonary venous Doppler indices for assessing murine left ventricular diastolic function. J Am Soc Echocardiogr. 2010; 23(8):887–897. doi: 10.1016/j.echo.2010.05.017. [PubMed: 20591622]

Zhang R, Lahens N, Ballance H, Hughes M, Hogenesch J. A circadian gene expression atlas in mammals: implications for biology and medicine. Proc Natl Acad Sci. 2014 In Press.

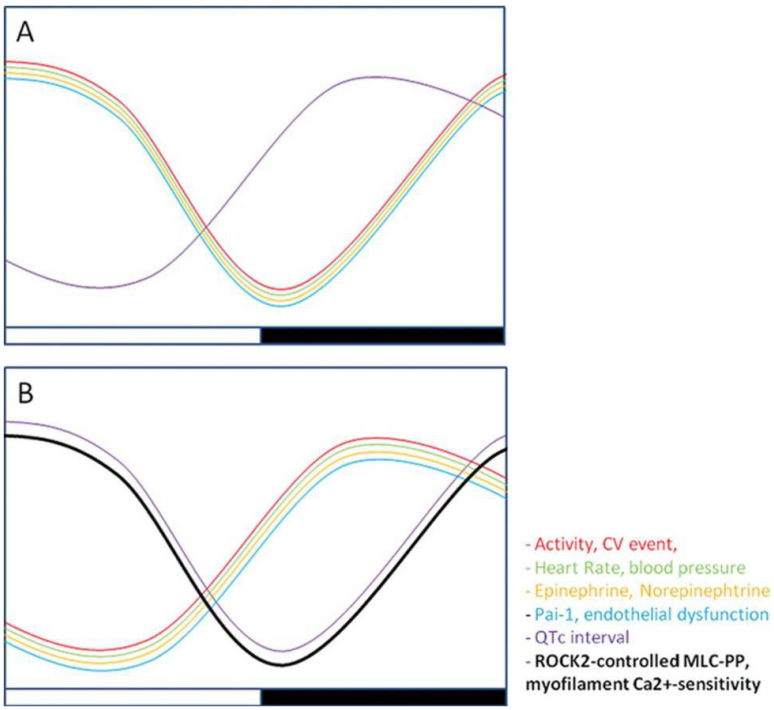

Figure 1.

Antiphasic circadian variation of the cardiovascular system in diurnal and nocturnal mammals. Cardiovascular events peak in the early morning in humans (A) correlating with a peak in process such as heart rate, blood pressure, and endothelial function. In nocturnal animals (B), such as mice, these occur at the start of the dark phase. CV indicates cardiovascular; Pai-1, plasminogen activator inhibitor-1; and QTc, corrected QT interval. Reproduced from (McLoughlin & FitzGerald, 2013).

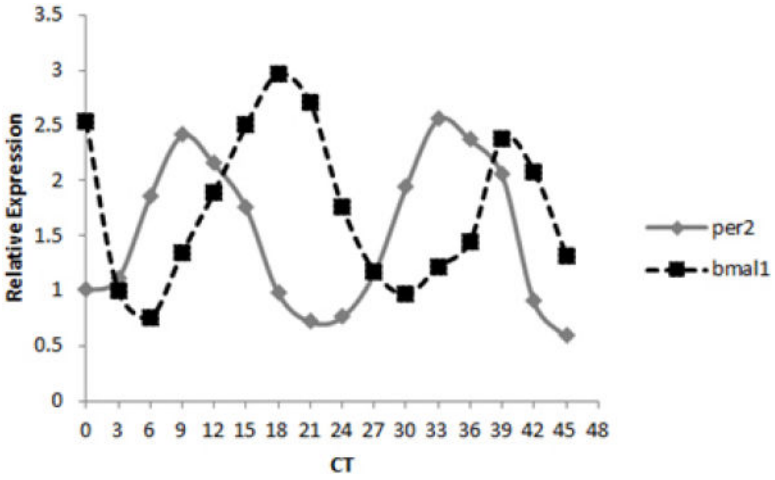

Figure 2.

Clock gene expression cycles in cultured peritoneal macrophages. Peritoneal cells cultured for several days were synchronized with dexamethasone and after 24 h were harvested every 3 h for two cycles. Clock genes *Per2* and *Bmal1* cycle in an antiphasic manner.

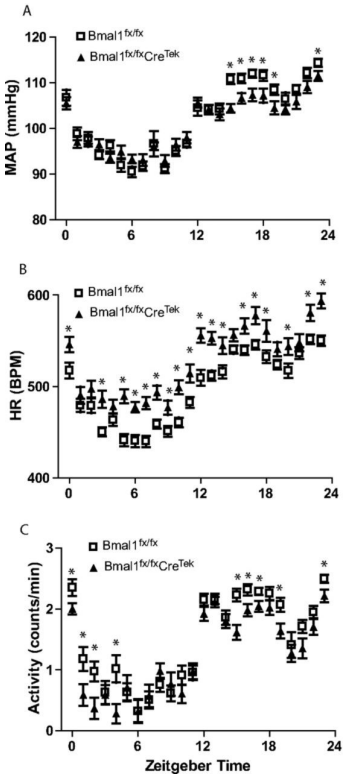

Figure 3.

Radiotelemetry is ideal for continuous recording of physiological events. Telemetric recordings for mean arteriole pressure (MAP, A), heart rate (HR, B), and activity (C) in *Bmal1*$^{fx/fx}$ and *Bmal1*$^{fx/fx}$*Cre*^{Tek} mice indicate that depression of BMAL1 in endothelial cells alters BP, HR, and activity. Plotted are the averages of each hour for three consecutive 24-h periods in 12:12 LD. (*P<0.05). Reproduced from Westgate et al (Westgate et al., 2008).

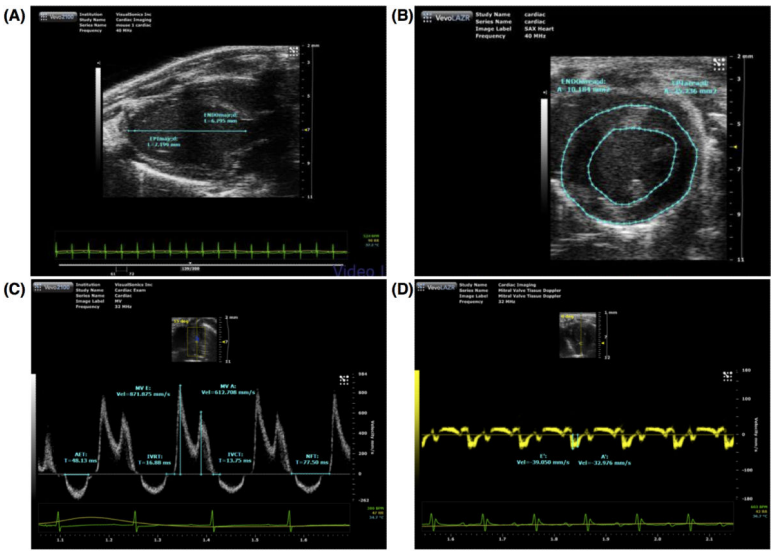

Figure 4.

Evaluation of systolic and diastolic function using in-vivo echocardiography (A) Parasternal long-axis view (B) 2-D short axis view (C) Transmitral pulse wave Doppler interrogation (D) Tissue doppler evaluation of myocardial relaxation. With permission from Tao Wang, Director Mouse Cardiovascular Physiology Core.